Extended data

NHEJ-mediated DNA synapsis and RPA-driven MRX exonuclease balance DNA end resection to control DSB repair pathway choice

Stefan Braunshier, Elda Cannavo, Ananya Acharya, Giordano Reginato,
Vincent Morin, Virginie Ropars, Raphael Guerois, Jean-Baptiste Charbonnier,
and Petr Cejka

This file contains:

- 8 Extended Data Figures with legends
- 2 Extended Data Tables

Extended Data Fig. 1

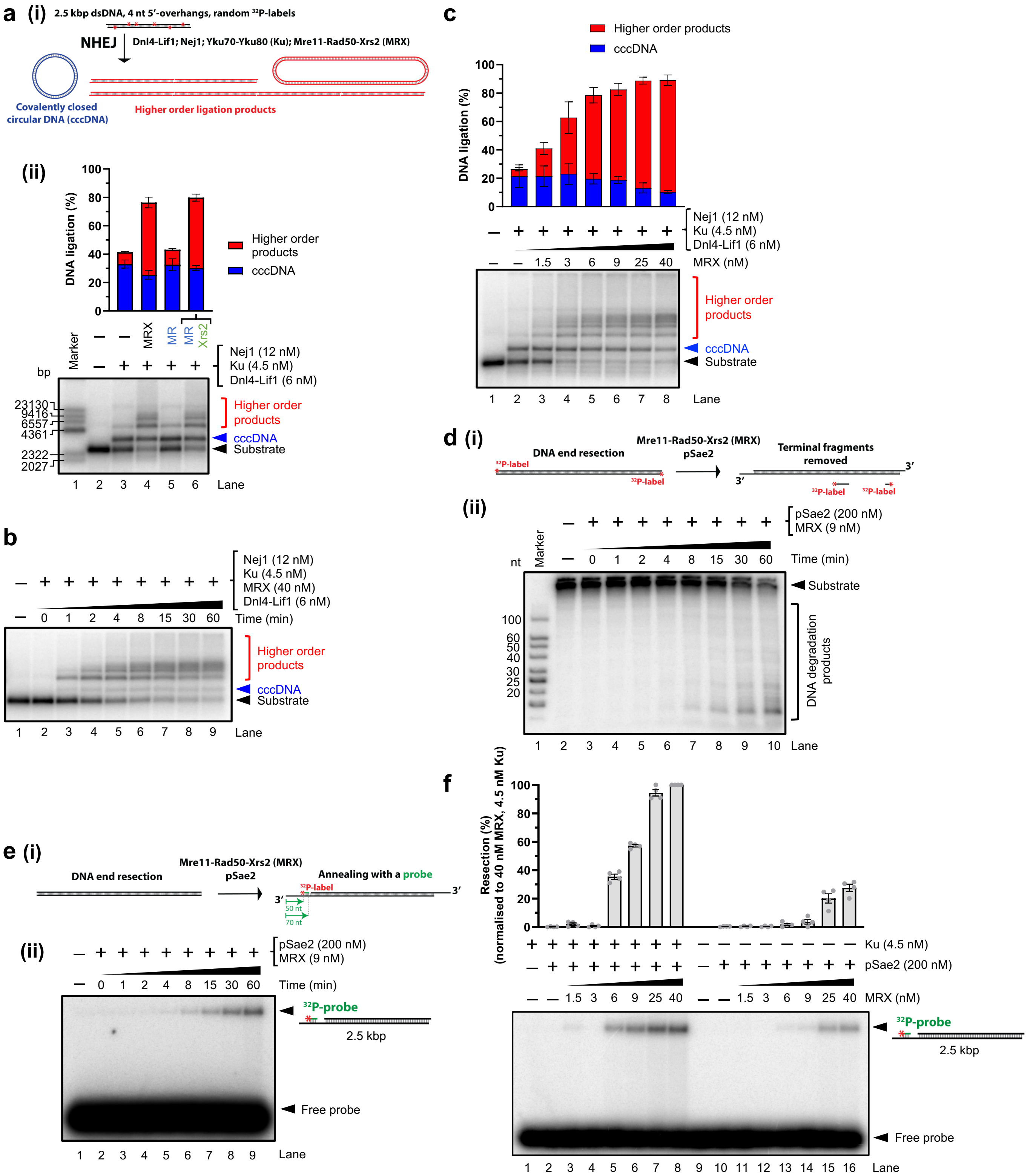

(Figure legend on the next page)

Extended Data Figure 1: Monitoring the efficacy of reconstituted NHEJ and DNA end resection assays.

a, Non-homologous end-joining assays with indicated proteins, and either MRX (9 nM), MR (9 nM) or MR (9 nM) added together with separately expressed Xrs2 (9 nM). **(i)** A schematic of the assay. Red asterisks (*) represent the random positions of the radioactive label. **(ii)** Top, quantitation of DNA ligation. Averages shown; error bars, s.e.m.; n = 4 for lanes 3 and 4 and n = 3 for lanes 5 and 6. Bottom, a representative image of three independent experiments. The products were separated on a 1.5% agarose gel in TAE.

b, Non-homologous end-joining assay as a kinetic experiment. The products were separated on a 1.5% agarose gel in TAE. A representative image of three independent experiments is shown.

c, Non-homologous end-joining assay and its dependence on MRX concentration. Top, quantitation of DNA ligation. Averages shown; error bars, s.e.m.; n = 3. Bottom, a representative image of three independent experiments is shown. The products were separated on a 1.5% agarose gel in TAE.

d, DNA end resection assays with 5′ terminally labeled DNA as a kinetic experiment. **(i)** A schematic of the assay. The red asterisk (*) represents the position of the radioactive label. **(ii)** A representative image of three independent experiments. The products were separated on a 15% denaturing polyacrylamide gel in TBE.

e, DNA end resection assay, monitored by oligonucleotide annealing, as a kinetic experiment. **(i)** A schematic of the assay. The red asterisk (*) represents the position of the radioactive label. **(ii)** A representative image of three independent experiments. The ssDNA probe was complementary to a region 50-70 bp away from the DNA end. The products were separated on a 1% agarose gel in TAE.

f, DNA end resection assay, monitored by oligonucleotide annealing, as a function of MRX concentration, in the presence or absence of Ku. Top, quantitation of DNA resection. Values were normalized to lane 8. Averages shown; error bars, s.e.m.; n = 4. Bottom, a representative image of four independent experiments. The ssDNA probe was complementary to a region 50-70 bp away from the DNA end. The products were separated on a 1% agarose gel in TAE.

Extended Data Fig. 2

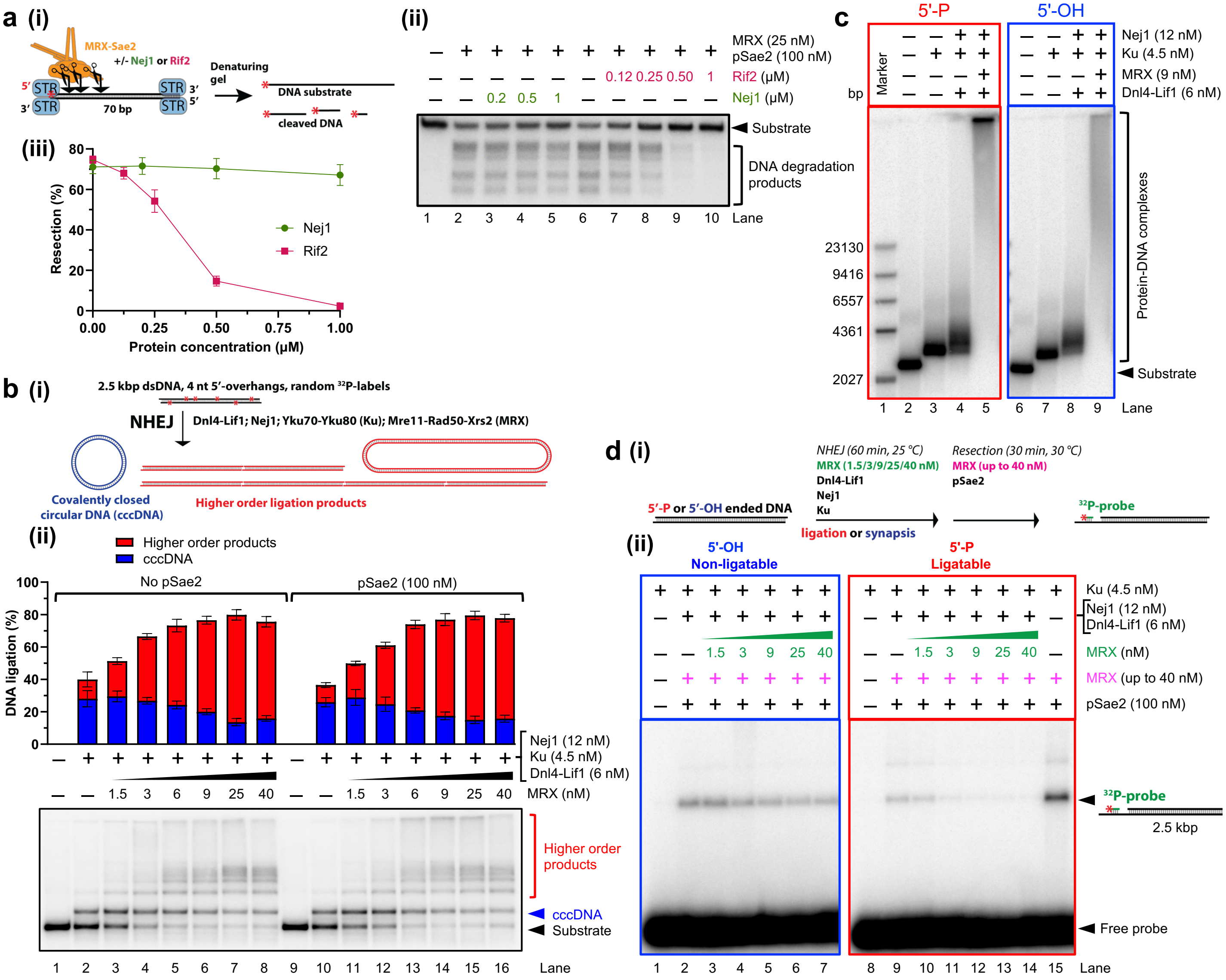

Extended Data Figure 2: Interplay of non-homologous end-joining and DNA end resection.

a, Endonuclease assays monitoring MRX-pSae2-mediated incision of end-blocked dsDNA in the presence or absence of Nej1 or Rif2. **(i)** A schematic of endonuclease assay with end-blocked 70 bp-long dsDNA and MRX-pSae2. The red asterisk (*) represents the position of the radioactive label. **(ii)** A representative image of three independent experiments. The products were separated on a 15% denaturing polyacrylamide gel in TBE. **(iii)** Quantitation of DNA resection from experiments such as in **(ii)**. Averages shown; error bars, s.e.m.; n = 3.

b, Phosphorylated Sae2 does not affect end-joining. **(i)** A schematic of the end-joining assay. Red asterisks (*) represent the random positions of the radioactive label. **(ii)** A representative image of three independent experiments. The products were separated on a 1.5% agarose gel in TAE.

c, Electrophoretic mobility shift assays with the indicated proteins and dsDNA containing either ligatable or non-ligatable DNA ends. The products were separated on a 0.6% agarose gel in TAE. A representative image of three independent experiments is shown.

d, Impact of NHEJ assembly on DNA end resection. **(i)** A schematic of the oligonucleotide annealing assay used to monitor resection after end-joining of DNA molecules with ligatable or non-ligatable DNA ends, with various MRX protein concentrations. **(ii)** A representative image of three independent experiments. Resection was analyzed with a probe complementary to a region 50-70 bp away from the DNA end.

Extended Data Fig. 3

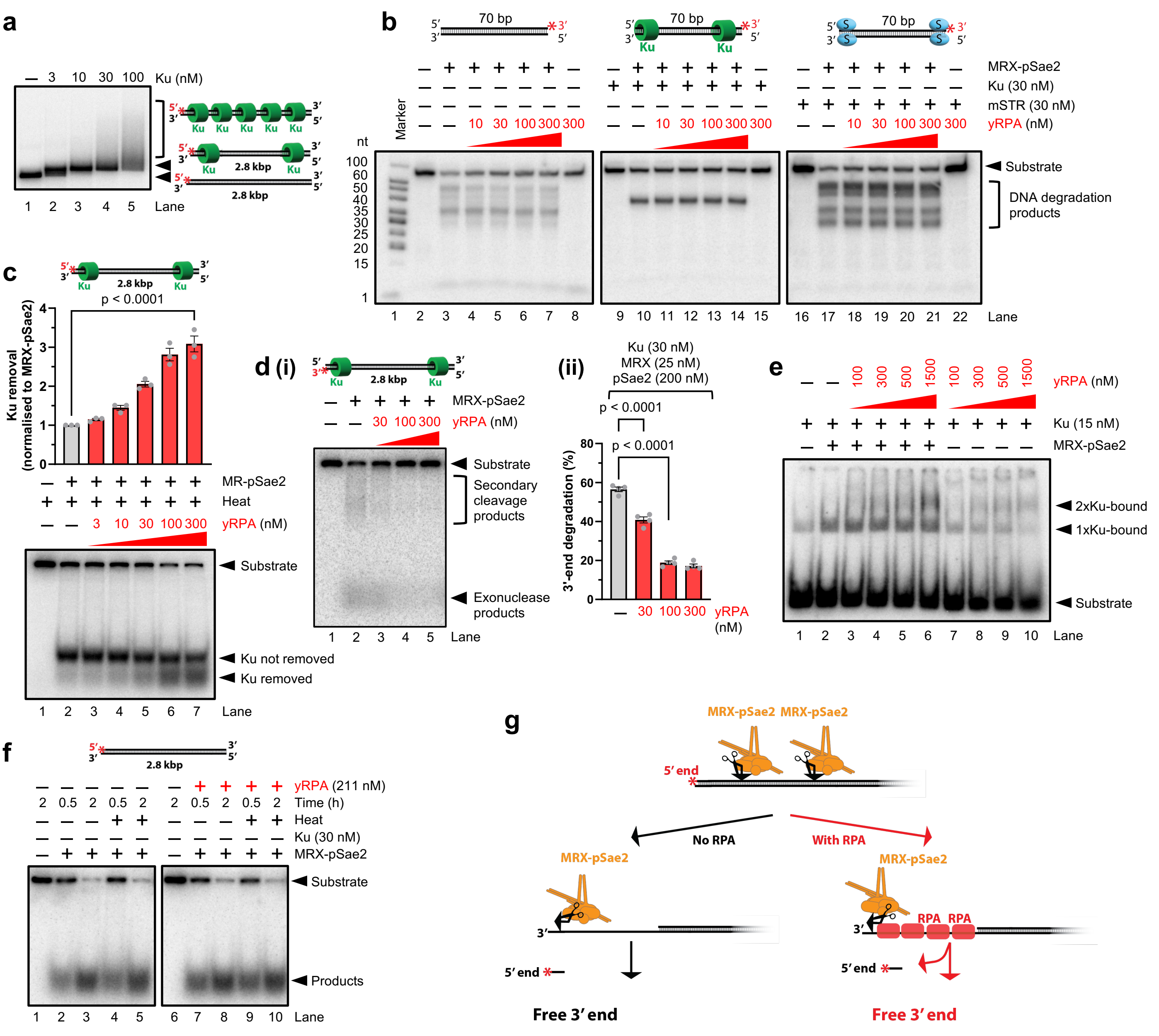

(Figure legend on the next page)

Extended Data Figure 3: Effect of RPA on the activities of the MR and MRX complexes.

a, DNA binding of Ku to dsDNA, monitored by electrophoretic mobility shift assay. A representative image of two independent experiments. The products were separated on a 0.6% agarose gel in TAE. The red asterisk (*) represents the position of the radioactive label.

b, RPA has no effect on the endonuclease activity of MRX (25 nM)-pSae2 (200 nM). Top, a cartoon of the substrates used. The position of monovalent streptavidin is marked with an S. The red asterisk (*) represent the positions of the radioactive labels. Bottom, a representative image of three independent experiments. The products were separated on 15% denaturing polyacrylamide gels. Monovalent streptavidin (mSTR).

c, The effect of RPA concentration on Ku removal by MR (25 nM)-pSae2 (200 nM) from DNA ends. Top, a cartoon of the substrate used. The red asterisk (*) represents the position of the radioactive label. Middle, quantitation of Ku removal by MR-pSae2. Values were normalized to lane 2. Averages shown; error bars, s.e.m.; n = 3. Statistical analysis was performed using Šídák's multiple comparisons test. Bottom, a representative image of three independent experiments. The products were separated on 10% native polyacrylamide gels in TAE.

d, RPA protects the 3′-end from degradation by MRX (25 nM)-pSae2 (200 nM). **(i)** Top, a cartoon of the substrate used. The red asterisk (*) represents the position of the radioactive label. Bottom, a representative image of three independent experiments. The products were separated on 10% native polyacrylamide gels in TAE. **(ii)** Quantitation of 3′ end degradation in experiments such as shown in **(i)**. Averages shown; error bars, s.e.m.; n = 4. Statistical analysis was performed using Šídák's multiple comparisons test.

e, Ku capture experiment showing Ku removal from a blunt-ended unlabeled 2.8 kbp-long dsDNA by MRX (25 nM)-pSae2 (200 nM), in the presence of various concentrations of RPA. Ku displacement is monitored by binding to a radioactively labeled trap. A representative image of four independent experiments is shown. For quantitation and cartoon of the assay, see Fig. 4h (i).

f, RPA has no effect on the processing of DNA ends by MRX (25 nM)-pSae2 (200 nM) in the absence of Ku. Top, a cartoon of the substrate used. The red asterisk (*) represents the position of the radioactive label. Bottom, a representative image of three independent experiments. The reaction products were separated on 10% native polyacrylamide gels in TAE.

g, A cartoon showing that MRX-pSae2 can efficiently process DNA ends without Ku, to produce free 3′-ends. The addition of RPA does not impact the reaction.

Extended Data Fig. 4

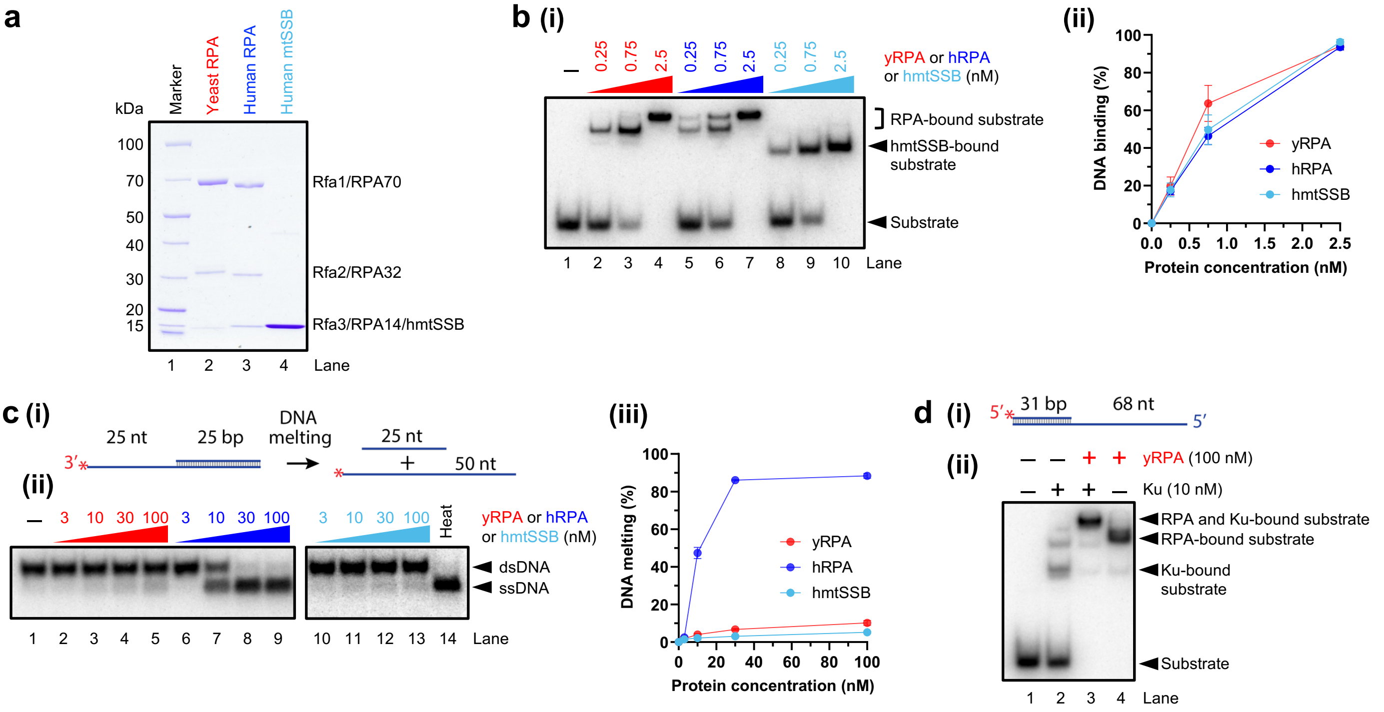

Extended Data Figure 4: Interplay of MRX-pSae2 with yeast RPA and non-cognate variants.

a, Recombinant yeast and human RPA proteins (yRPA, hRPA) and human mitochondrial SSB (hmtSSB) used in this study. The polyacrylamide gel was stained with Coomassie Brilliant Blue.

b, Electrophoretic mobility shift assays monitoring the binding of 50 nt-long ssDNA by yeast RPA (yRPA), human RPA (hRPA) and human mitochondrial SSB (hmtSSB) to ssDNA. The products were separated on 6% native polyacrylamide gels in TAE. **(i)** A representative image of three independent experiments. **(ii)** Quantitation of ssDNA binding by yRPA, hRPA and hmtSSB from experiment such as shown in **(i)**. Averages shown; error bars, s.e.m.; n = 3.

c, DNA melting by yRPA, hRPA and hmtSSB. **(i)** A cartoon of the substrate used. The red asterisk (*) represents the position of the radioactive label. **(ii)** A representative image of three independent experiments. The products were separated on 8% native polyacrylamide gels in TBE. **(iii)** Quantitation of DNA melting from experiments such shown in **(ii)**. Averages shown; error bars, s.e.m.; n = 3.

d, RPA alone does not displace Ku from 5′-overhanged DNA. **(i)** A cartoon of the substrate used. The red asterisk (*) represents the position of the radioactive label. **(ii)** Electrophoretic mobility shift assays with yeast RPA and Ku and a 5′-overhanged substrate. The products were separated on 4% native polyacrylamide gels in TAE. A representative image of three independent experiments is shown. RPA and Ku can bind the DNA substrate simultaneously.

Extended Data Fig. 5

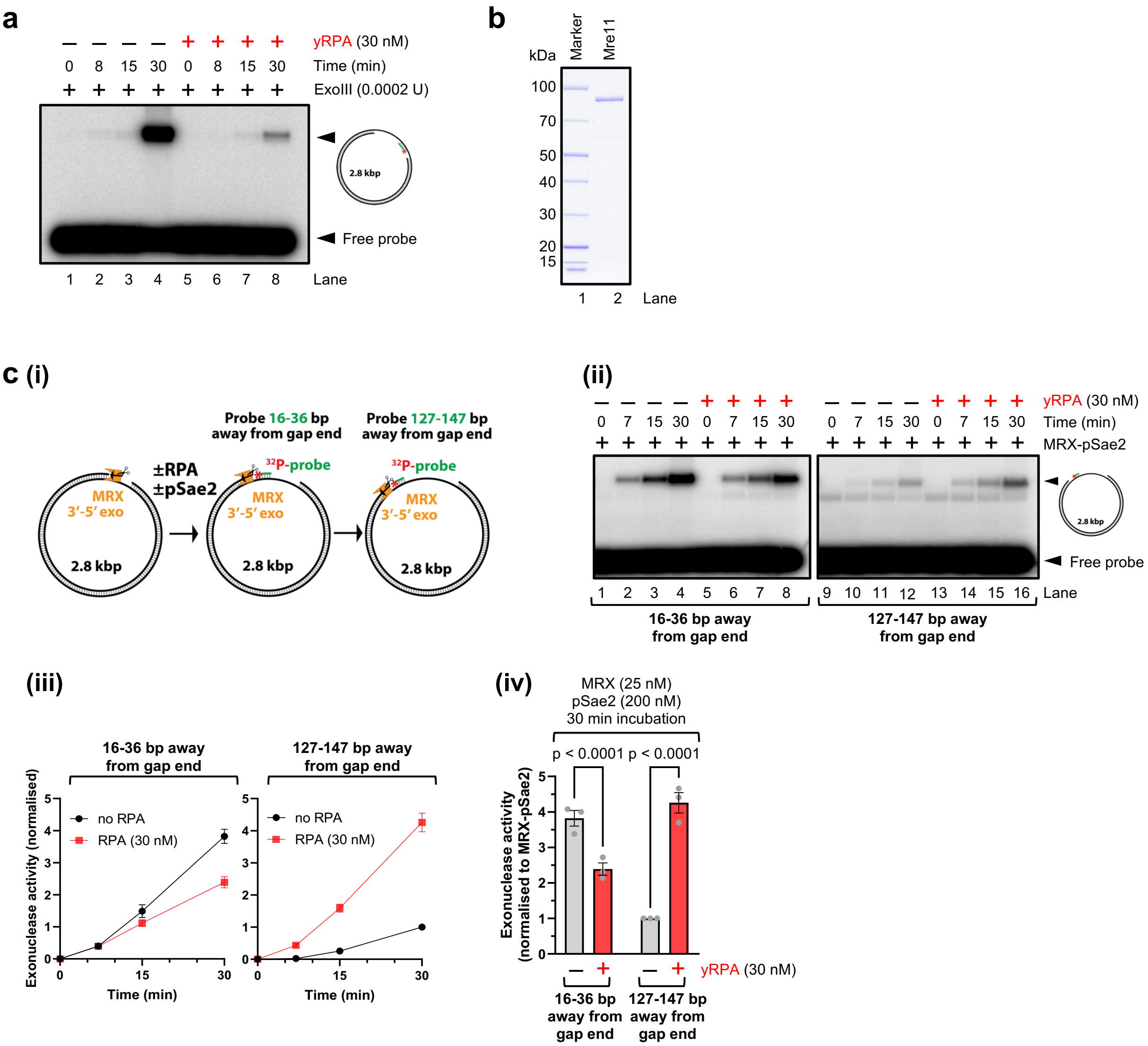

Extended Data Figure 5: RPA stimulates the processivity of the MRX-pSae2 exonuclease in a species-specific manner

a, The exonuclease activity of ExoIII is inhibited by yeast RPA (yRPA). Oligonucleotide annealing assay used to monitor the 3′-5′ exonuclease activity of *E. coli* ExoIII on a gapped plasmid, probed 127-147 bp away from the gap, in the presence or absence of yeast RPA. The products were separated on a 1% agarose gel in TAE. A representative image of three independent experiments is shown.

b, Recombinant yeast Mre11 used in this study. The polyacrylamide gel was stained with Coomassie Brilliant Blue.

c, Oligonucleotide annealing assay used to monitor the exonuclease activity of MRX (25 nM)-pSae2 (200 nM) on a gapped plasmid, probed either 16-36 or 127-147 bp away from the gap, in the presence or absence of yeast RPA. The products were separated on a 1% agarose gel in TAE. **(i)** A schematic of the oligonucleotide annealing assays shown in **(ii)**. The exonuclease activity of MRX-pSae2, and the effect of RPA, was monitored in proximity to the gap (16-36 bp away) or further away from the gap (127-147 bp). **(ii)** A representative image of three independent experiments is shown. **(iii)** Quantitation of the exonuclease activity of MRX-pSae2, with or without RPA, from experiments such as shown in **(ii)** shown as a function of time. **(iv)** Quantitation of the exonuclease activity of MRX-pSae2, with or without RPA after 30 min of incubation. Values were normalized to lane 12 (MRX-pSae2 alone without RPA, probe 16-36 bp away from the gap). Averages shown; error bars, s.e.m.; n = 3. Statistical analysis was performed using Šídák's multiple comparisons test.

Extended Data Fig. 6

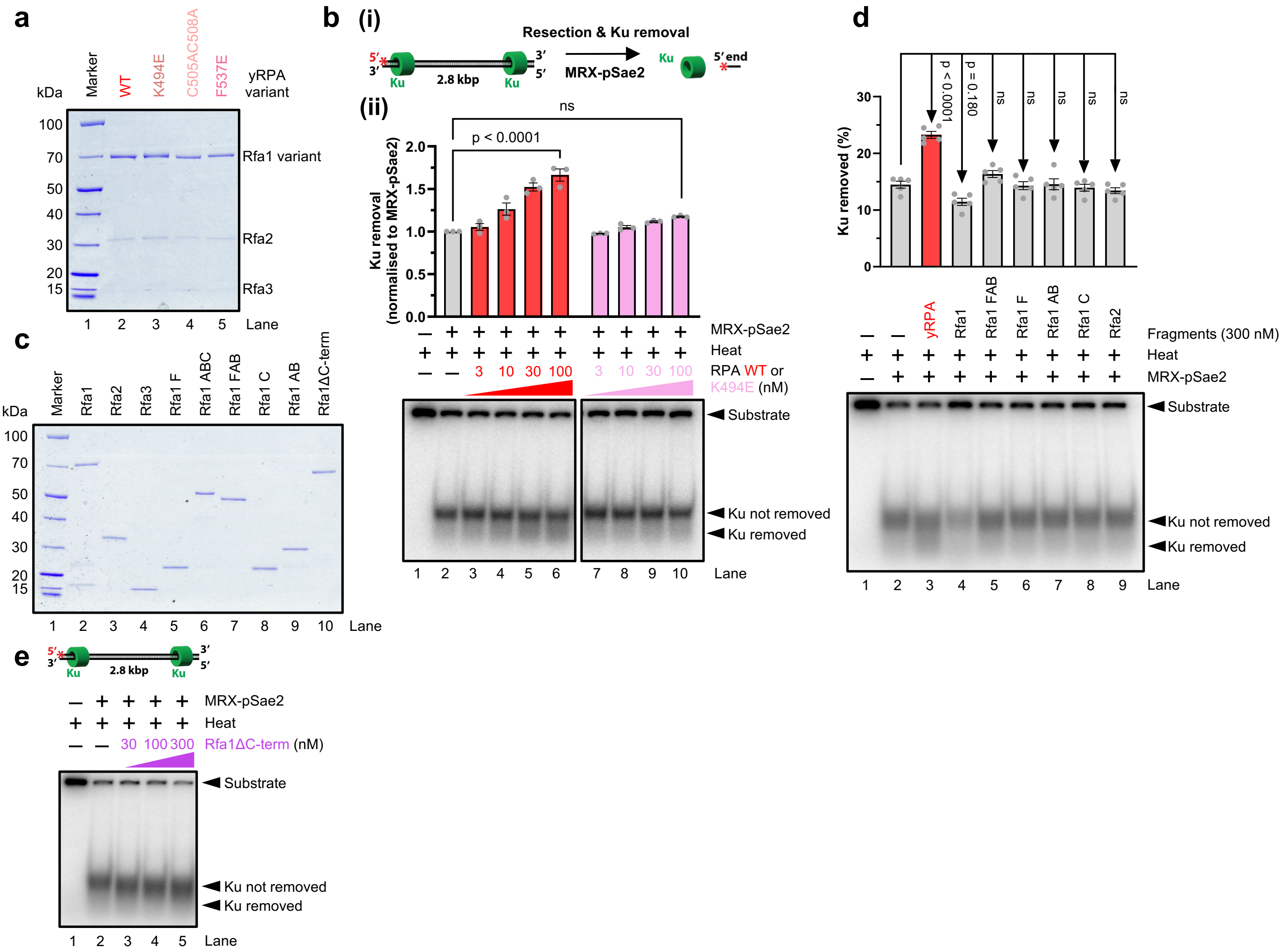

Extended Data Figure 6: Effect of various RPA variants on the exonuclease activity of MRX-pSae2.

a, Yeast RPA point mutants used in this study. The polyacrylamide gel was stained with Coomassie Brilliant Blue.

b, DNA binding-deficient RPA variant fails to assist MRX (25 nM)-pSae2 (200 nM) in removing Ku from DNA ends. **(i)** A cartoon of the assay. The red asterisk (*) represents the position of the radioactive label. **(ii)** Top, quantitation of Ku removal by MRX-pSae2 and its stimulation by wild-type RPA or RPA K494E (mutation in the OB-C domain of the Rfa1 subunit). Values were normalized to lane 2 (Ku removal by MRX-pSae2 alone without RPA). Averages shown; error bars, s.e.m.; n = 3. Statistical analysis was performed using Šídák's multiple comparisons test; ns, not significant. Bottom, a representative image of three independent experiments. The products were separated on 10% native polyacrylamide gels in TAE.

c, Recombinant RPA fragments used in this study. The polyacrylamide gels were stained with Coomassie Brilliant Blue.

d, Ku removal by MRX (25 nM)-pSae2 (200 nM) and its stimulation by RPA fragments. Assay as in panel **b**. Top, quantitation of Ku removal by MRX-pSae2, calculated as a fraction of the "Ku removed" band vs. the rest of the lane. Averages shown; error bars, s.e.m.; n = 5. Statistical analysis was performed using Šídák's multiple comparisons test; ns, not significant. Bottom, a representative image of five independent experiments. The products were separated on 10% native polyacrylamide gels in TAE.

e, The effect of the C-terminal domain of Rfa1 on Ku removal by MRX (25 nM)-pSae2 (200 nM). Top, a cartoon of the substrate used. The red asterisk (*) represents the position of the radioactive label. Bottom, a representative image of four independent experiments. The products were separated on 10% native polyacrylamide gels in TAE.

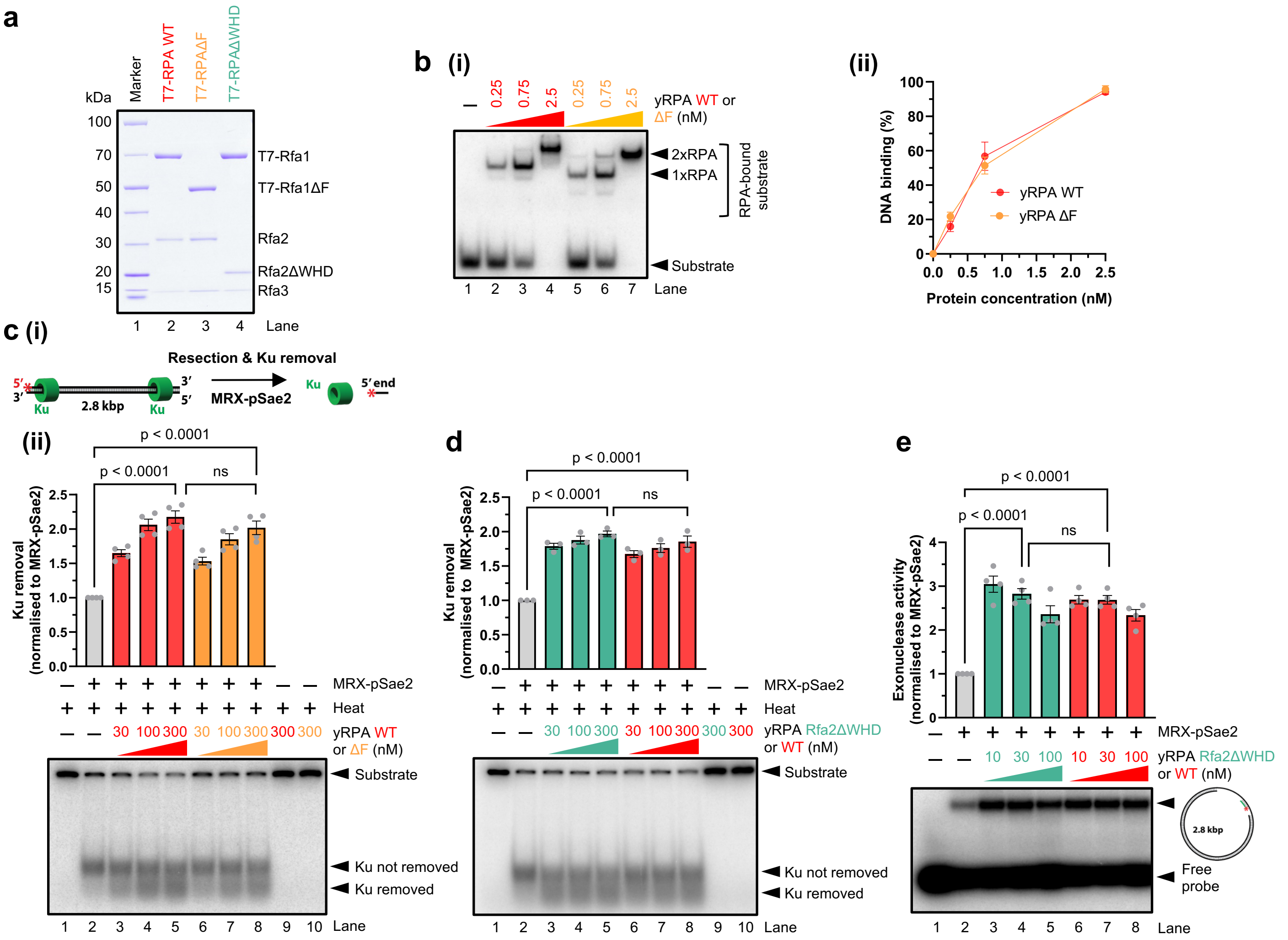

Extended Data Figure 7: Effect of OB-F domain of RPA on the exonuclease activity of MRX-pSae2.

a, RPA truncations used in this study. RPAΔF lacks N-terminal residues (1-180) of Rfa1, while RPAΔWHD lacks C-terminal residues (184-274) of Rfa2. The polyacrylamide gel was stained with Coomassie Brilliant Blue.

b, Truncation of the OB-F domain of Rfa1 does not affect its ssDNA binding affinity, as monitored by electrophoretic mobility shift assays. **(i)** A representative image of three independent experiments is shown. The products were separated on 6% native polyacrylamide gels in TAE. **(ii)**, Quantitation of ssDNA binding by RPA variants from experiments such as the one shown in **(i)**. Averages shown; error bars, s.e.m.; n = 3.

c, The OB-F domain of Rfa1 is not essential for MRX (25 nM)-pSae2 (200 nM)-mediated Ku removal. **(i)** A cartoon of the assay. Red asterisks (*) represent the position of the radioactive label. **(ii)** Top, quantitation of Ku removal by MRX-pSae2. Values were normalized to lane 2 (MRX-pSae2 alone without RPA). Averages shown; error bars, s.e.m.; n = 4. Statistical analysis was performed using Šídák's multiple comparisons test; ns, not significant. Bottom, a representative image of four independent experiments is shown. The products were separated on 10% native polyacrylamide gels in TAE.

d, The C-terminal WHD domain of Rfa2 is dispensable for the stimulation of Ku removal by MRX (25 nM)-pSae2 (200 nM). Assay as in panel **c**. Top, quantitation of Ku removal by MRX-pSae2. Values were normalized to lane 2 (MRX-pSae2 alone without RPA). Averages shown; error bars, s.e.m.; n = 3. Statistical analysis was performed using Šídák's multiple comparisons test; ns, not significant. Bottom, a representative image of three independent experiments is shown. The products were separated on 10% native polyacrylamide gels in TAE.

e, The Rfa2ΔWHD truncation of RPA does not affect the stimulation of the exonuclease activity of MRX (25 nM)-pSae2 (200 nM) on a gapped plasmid, monitored using the oligonucleotide annealing assay. Top, quantitation of the exonuclease activity of MRX-pSae2 on a gapped plasmid, probed 127-147 bp away from the gap. Values were normalized to lane 2 (MRX-pSae2 alone without RPA). Averages shown; error bars, s.e.m.; n = 4. Statistical analysis was performed using Šídák's multiple comparisons test; ns, not significant. Bottom, a representative image of four independent experiments is shown. The products were separated on a 1% agarose gel in TAE.

Extended Data Fig. 8

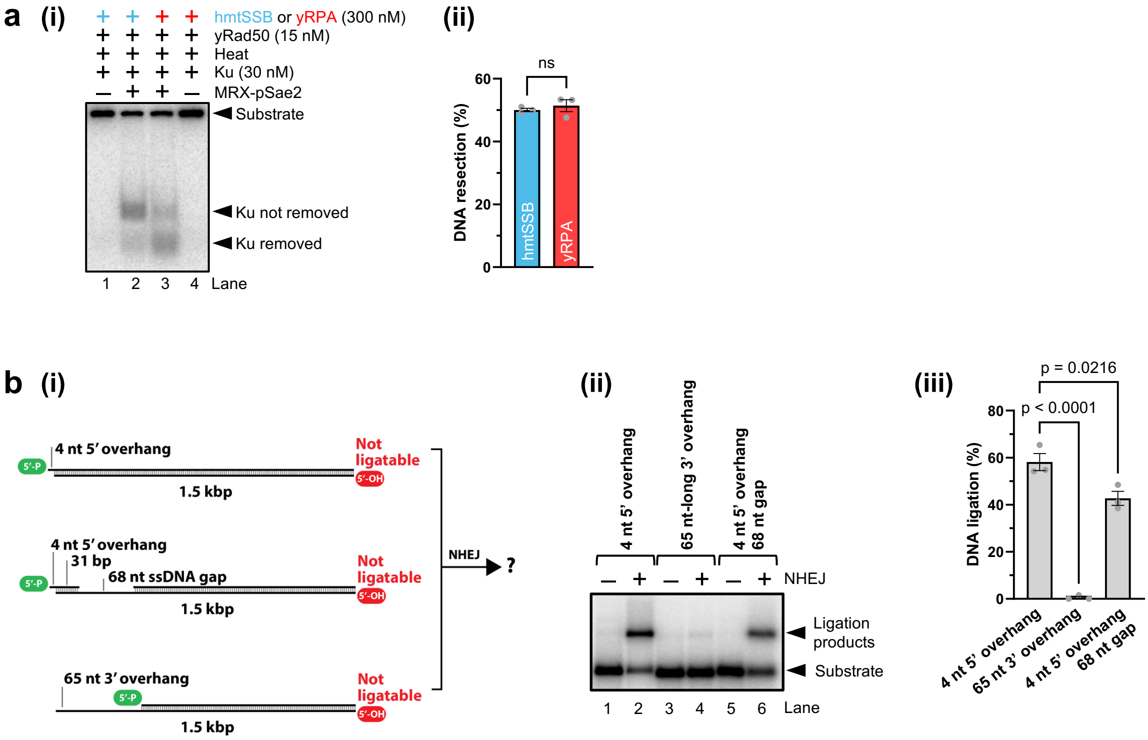

Extended Data Figure 8: Internal gaps at DSBs limit but do not eliminate NHEJ.

a, The efficiency of DNA end resection by MRX-pSae2 under assay conditions as in Fig. 8b. yRPA and hmtSSB do not affect DNA incision by MRX-pSae2. **(i)** MRX (25 nM) and pSae2 (200 nM)-mediated resection and Ku removal assay on a 5'-labeled 1.5 kbp-long PCR, in the presence of yRPA or hmtSSB. The products were separated on 10% native polyacrylamide gels in TAE. A representative image of three independent experiments is shown. **(ii)** Quantitation of DNA resection efficiency (calculated as substrate utilization) from the experiments such as shown in **(i)**. Averages shown; error bars, s.e.m.; n = 3. Statistical analysis was performed using Šídák's multiple comparisons test; ns, not significant.

b, Internally gapped DNA is ligatable by NHEJ. **(i)** A cartoon of the substrates representing resection intermediates, that were tested for end-joining. **(ii)** End-joining assay of resection intermediates. The products were separated on a 1.5% agarose gels in TAE. A representative image of three independent experiments is shown. **(iii)** Quantitation of DNA ligation efficiency from the experiments such as shown in **(ii)**. Averages shown; error bars, s.e.m.; n = 3. Statistical analysis was performed using Šídák's multiple comparisons test.

Extended Data Table 1: Oligonucleotides used for substrate preparation in this study.

[B] and [TB] represent the positions of biotin modifications in the DNA.

Oligonucleotide name	DNA sequence
PC209	GATGCATGAGGTGGAGTACGCGCCCGGGGAGCCCAAGGGCACGCCCTGGCACCCGCACCGCGGCACT[TB]AC
PC210	G[TB]AAGTGCCGCGGTGCGGGTGCCAGGGCGTGCCCTTGGGCTCCCCGGGCGCGTACTCCACCTCATGCA[TB]C
PC211	GA[TB]GCATGAGGTGGAGTACGCGCCCGGGGAGCCCAAGGGCACGCCCTGGCACCCGCACCGCGGCACT[TB]AC
PC216	GTAAGTGCCGCGGTGCGGGTGCCAGGGCGTGCCCTTGGGCTCCCCGGGCGCGTACTCCACCTCATGCATC
PC1253	TGGGTCAACGTGGGCAAAGATGTCCTAGCAATGTAATCGTCTATGACGTT
PC1255	GTCGGATCCTCTAGACAGCTCCATGATCACTGGCACTGGTAGAATTCGGC
314	CATGGAGCTGTCTAGAGGATCCGAC
X12-4SC	GCGATAGTCTCTAGACAGCATGTCCTAGCAA
X12-3L	AACACCTACTATCCCACGAGCAGAGCTGATTCTTACAAATATGATTCGAGACGTCATAGACGATTACATTGCTAGGACATGCTGTCTAGAGACTATCGC
3'-100	GGCGGCTCGTATGTTGTGTGGA
INT 5'-0	GGGTAAGTGCCGCGGTGCGGGTG
INT 5'-40	GGTTCTCTCAGTTGGGGGCGTAG
V2 3'-100 TOP	GGGCTGCAAGGCGATTAAGTTG
V2 3'-15 TOP	GGACTGAGCCTCTCGACTTCAC
70BP-NHEJ-PUC19TN	GGCCGTCGTTTTACAACGT
CAG_X4_bottom_strand_biotin	[B]CGTATCTTACCGGGTTGGATTCAAGACGATAGTTAAGCAGTTGAACGACTGAGCGCAGCGACTCTGACGT[B]
Top strand oligo WT FRP	ACGTCAGAGTCGCTGCGCTCAGTCGTTCAACTGCTTAACTATCGTCTTGAATCCAACCCGGTAAGATACG
WHDv2_197mer_bot	GCGAGTGGTCGGCAGATTGCGATAAACGGTCACATTAAATTTAACCTGACTATTCCACTGCAACAACTGAACGGACTGGAAACACTGGTCATAATCATGGTGGCGAATAAGTACGCGTTCTTGCAAATCACCAGAAGGCGGTTCCTGAATGAATGGGAAGCCTTCAAGAAGGTGATAAGCAGGAGAAACATACGAAG
WHDv2_196mer_B_top	[B]GCTTCGTATGTTTCTCCTGCTTATCACCTTCTTGAAGGCTTCCCATTCATTCAGGAACCGCCTTCTGGTGATTTGCAAGAACGCGTACTTATTCGCCACCATGATTATGACCAGTGTTTCCAGTCCGTTCAGTTGTTGCAGTGGAATAGTCAGGTTAAATTTAATGTGACCGTTTATCGCAATCTGCCGACCACTCG

Extended Data Table 2: The sequence of the pG68v2 plasmid

TCGCGCGTTTCGGTGATGACGGTGAAAACCTCTGACACATGCAGCTCCCGGAGACGGTCACAGCTTGTCTGTAAGCGGATGCCGGGAGCAGACAAGCCCGTCAGGGCGCGTCAGCGGGTGTTGGCGGGTGTCGGGGCTGGCTTAACTATGCGGCATCAGAGCAGATTGTACTGAGAGTGCACCATATGCGGTGTGAAATACCGCACAGATGCGTAAGGAGAAAATACCGCATCAGGCGCCATTCGCCATTCAGGCTGCGCAACTGTTGGGAAGGGCGATCGGTGCGGGCCTCTTCGCTATTACGCCAGCTGGCGAAAGGGGGATGTGCTGCAAGGCGATTAAGTTGGGTAACGCCAGGGTTTTCCCAGTCACGACGTTGTAAAACGACGGCCAGTGCCAAGCTTAGTCTGCTGCCCTTAGGCCATGGAGCTTCACTCACTGAGCCTCTCGACTTCACAAGTAGCTGCTCTTCCTCAGCACGTCCTCAGCTACACCTCAGCGATCCCTCAGCACTAGTCCTCAGCTACGCCTCAGCGATTCCTCAGCATATCCATGAGCCTGTCACCCTAGGCGGCTGCCTGCGCATCCTGGGATCCGGGAAGCCAGAGATGAGGCGAATTCGTAATCATGTCATAGCTGTTTCCTGTGTGAAATTGTTATCCGCTCACAATTCCACACAACATACGAGCCGGAAGCATAAAGTGTAAAGCCTGGGGTGCCTAATGAGTGAGCTAACTCACATTAATTGCGTTGCGCTCACTGCCCGCTTTCCAGTCGGGAAACCTGTCGTGCCAGCTGCATTAATGAATCGGCCAACGCGCGGGGAGAGGCGGTTTGCGTATTGGGCGGTCTTCCGCTTCCTCGCTCACTGACTCGCTGCGCTCGGTCGTTCGGCTGCGGCGAGCGGTATCAGCTCACTCAAAGGCGGTAATACGGTTATCCACAGAATCAGGGGATAACGCAGGAAAGAACATGTGAGCAAAAGGCCAGCAAAAGGCCAGGAACCGTAAAAAGGCCGCGTTGCTGGCGTTTTTCCATAGGCTCCGCCCCCCTGACGAGCATCACAAAAATCGACGCTCAAGTCAGAGGTGGCGAAACCCGACAGGACTATAAAGATACCAGGCGTTTCCCCCTGGAAGCTCCCTCGTGCGCTCTCCTGTTCCGACCCTGCCGCTTACCGGATACCTGTCCGCCTTTCTCCCTTCGGGAAGCGTGGCGCTTTCTCATAGCTCACGCTGTAGGTATCTCAGTTCGGTGTAGGTCGTTCGCTCCAAGCTGGGCTGTGTGCACGAACCCCCCGTTCAGCCCGACCGCTGCGCCTTATCCGGTAACTATCGTCTTGAGTCCAACCCGGTAAGACACGACTTATCGCCACTGGCAGCAGCCACTGGTAACAGGATTAGCAGAGCGAGGTATGTAGGCGGTGCTACAGAGTTCTTGAAGTGGTGGCCTAACTACGGCTACACTAGAAGAACAGTATTTGGTATCTGCGCTCTGCTGAAGCCAGTTACCTTCGGAAAAAGAGTTGGTAGCTCTTGATCCGGCAAACAAACCACCGCTGGTAGCGGTGGTTTTTTTGTTTGCAAGCAGCAGATTACGCGCAGAAAAAAAGGATCTCAAGAAGATCCTTTGATCTTTTCTACGGGGTCTGACGCTCAGTGGAACGAAAACTCACGTTAAGGGATTTTGGTCATGAGATTATCAAAAAGGATCTTCACCTAGATCCTTTTAAATTAAAAATGAAGTTTTAAATCAATCTAAAGTATATATGAGTAAACTTGGTCTGACAGTTACCAATGCTTAATCAGTGAGGCACCTATCTCAGCGATCTGTCTATTTCGTTCATCCATAGTTGCCTGACTCCCCGTCGTGTAGATAACTACGATACGGGAGGGCTTACCATCTGGCCCCAGTGCTGCAATGATACCGCGAGACCCACGCTCACCGGCTCCAGATTTATCAGCAATAAACCAGCCAGCCGGAAGGGCCGAGCGCAGAAGTGGTCCTGCAACTTTATCCGCCTCCATCCAGTCTATTAATTGTTGCCGGGAAGCTAGAGTAAGTAGTTCGCCAGTTAATAGTTTGCGCAACGTTGTTGCCATTGCTACAGGCATCGTGGTGTCACGCTCGTCGTTTGGTATGGCTTCATTCAGCTCCGGTTCCCAACGATCAAGGCGAGTTACATGATCCCCCATGTTGTGCAAAAAAGCGGTTAGCTCCTTCGGTCCTCCGATCGTTGTCAGAAGTAAGTTGGCCGCAGTGTTATCACTCATGGTTATGGCAGCACTGCATAATTCTCTTACTGTCATGCCATCCGTAAGATGCTTTTCTGTGACTGGTGAGTACTCAACCAAGTCATTCTGAGAATAGTGTATGCGGCGACCGAGTTGCTCTTGCCCGGCGTCAATACGGGATAATACCGCGCCACATAGCAGAACTTTAAAAGTGCTCATCATTGGAAAACGTTCTTCGGGGCGAAAACTCTCAAGGATCTTACCGCTGTTGAGATCCAGTTCGATGTAACCCACTCGTGCACCCAACTGATCTTCAGCATCTTTTACTTTCACCAGCGTTTCTGGGTGAGCAAAAACAGGAAGGCAAAATGCCGCAAAAAAGGGAATAAGGGCGACACGGAAATGTTGAATACTCATACTCTTCCTTTTTCAATATTATTGAAGCATTTATCAGGGTTATTGTCTCATGAGCGGATACATATTTGAATGTATTTAGAAAAATAAACAAATAGGGGTTCCGCGCACATTTCCCCGAAAAGTGCCACCTGACGTCTAAGAAACCATTATTATCATGACATTAACCTATAAAAATAGGCGTATCACGAGGCCCTTTCGTC